

# Rationally designed PKA inhibitors for positron emission tomography: Synthesis and cerebral biodistribution of *N*-(2-(4-bromocinnamylamino)ethyl)-*N*-[<sup>11</sup>C]methyl-isoquinoline-5-sulfonamide

Neil Vasdev,<sup>a,b,\*</sup> Frank J. LaRonde,<sup>c</sup> James R. Woodgett,<sup>d,e</sup> Armando Garcia,<sup>a</sup> Elizabeth A. Rubie,<sup>e</sup> Jeffrey H. Meyer,<sup>a,b</sup> Sylvain Houle<sup>a,b</sup> and Alan A. Wilson<sup>a,b</sup>

<sup>a</sup>Centre for Addiction and Mental Health, 250 College Street, Toronto, Ont., Canada M5T 1R8

<sup>b</sup>Department of Psychiatry, University of Toronto, 250 College Street, Toronto, Ont., Canada M5T 1R8

<sup>c</sup>Laro Chemicals, 218 Queens Quay W., Suite 902, Toronto, Ont., Canada M5J 2Y6

<sup>d</sup>Department of Medical Biophysics, University of Toronto, 1 King's College Circle, Toronto, Ont., Canada M5S 1A8

<sup>e</sup>Ontario Cancer Institute/Princess Margaret Hospital, 610 University Avenue, Toronto, Ont., Canada M5G 2M9

Received 20 November 2007; revised 27 February 2008; accepted 3 March 2008

Available online 6 March 2008

**Abstract**—Protein kinase A (PKA) is an important signal transduction target for drug development because it influences critical cellular processes implicated in neuropsychiatric illnesses such as major depressive disorder. The goal of the present study was to develop the first imaging agent for measuring the levels of PKA with positron emission tomography (PET). By rational derivatization of 5-isoquinoline sulfonamides, it was found that the introduction of a methyl group to the sulphonamidic nitrogen on the known PKA inhibitors *N*-(2-aminoethyl)isoquinoline-5-sulfonamide (H-9, **1**) and *N*-(2-(4-bromocinnamylamino)ethyl)isoquinoline-5-sulfonamide (H-89, **2**), (yielding *N*-(2-aminoethyl)-*N*-methyl-isoquinoline-5-sulfonamide (**4**) and *N*-(2-(4-bromocinnamylamino)ethyl)-*N*-methyl-isoquinoline-5-sulfonamide (**5**), respectively) does not appreciably reduce in vitro potency toward PKA. We have facilitated the synthesis of **4** by reacting isoquinoline-5-sulfonyl chloride with *N*-methylethylenediamine (20% yield). Several techniques were used to thoroughly characterize **4** including multi (<sup>1</sup>H, <sup>13</sup>C and <sup>15</sup>N) NMR spectroscopy and X-ray crystallography. Compound **4** and 1-(4-bromophenyl)-1-propen-3-yl bromide were reacted to produce **5** in 16% yield. Compound **2** was reacted with [<sup>11</sup>C]CH<sub>3</sub>I to prepare *N*-(2-(4-bromocinnamylamino)ethyl)-*N*-[<sup>11</sup>C]methyl-isoquinoline-5-sulfonamide ([<sup>11</sup>C]**5**), with a decay-corrected radiochemical yield of 32%, based on [<sup>11</sup>C]CO<sub>2</sub>. [<sup>11</sup>C]**5** was produced with >98% radiochemical purity and 1130 mCi/μmol specific activity after 40 min (end of synthesis). Conscious rats were administered [<sup>11</sup>C] **5** and sacrificed at 5, 15, 30 and 60 min after injection. Radioactivity from all excised brain regions was <0.2%ID/g at all time points. The modest brain penetration of [<sup>11</sup>C]**5** may limit its use for studying PKA in the central nervous system.

© 2008 Elsevier Ltd. All rights reserved.

## 1. Introduction

Protein kinases have emerged to become an important class of drug targets<sup>1</sup> because they influence a number of key cellular processes such as neurotransmitter release, cell growth, and gene transcription. Rapid development of small molecule protein kinase inhibitors in drug discovery and signal transduction therapy is under-

way and well documented.<sup>2</sup> Among the protein kinases, protein kinase A (PKA) is particularly intriguing for neuropsychiatric drug development because it is a major mediator of response to cyclic adenosine monophosphate (cAMP), an intracellular second messenger utilized by many hormones and neurotransmitter binding receptors.<sup>3,4</sup> Interventions upon cerebral PKA function have been considered in the therapeutics of neuropsychiatric illnesses such as Alzheimer's disease, Parkinson's disease, mild cognitive impairment, schizophrenia, and in particular, major depressive disorder (MDD).<sup>5</sup> In MDD, PKA dysfunction has been identified in the pathophysiology of the illness: both reduced expression and activity of PKA subunits were identified in the

**Keywords:** Carbon-11; PET; H-89; H-9; Protein kinase A; Signal transduction.

\* Corresponding author. Tel.: +1 416 5358501x4680; fax: +1 416 9794656; e-mail: [neil.vasdev@camhpet.ca](mailto:neil.vasdev@camhpet.ca)

prefrontal cortex of depressed suicide victims,<sup>6,7</sup> and antidepressant medications raise levels of PKA in prefrontal cortex of rodents.<sup>5</sup> Given these findings, it is unsurprising that dysfunction of PKA is viewed as a central component in the models of aberrant intracellular signaling in MDD.

Positron emission tomography (PET) is a powerful, non-invasive method for imaging biological targets and processes in living subjects.<sup>8</sup> Quantitation of PKA levels could be achieved with PET, provided a suitable radiotracer was available. However, limited success has been made in the development of radiotracers for imaging cerebral signal transduction with PET. Human brain-PET studies of signal transduction have been achieved with carbon-11 (<sup>11</sup>C; half-life = 20.4 min) labeled Rolipram,<sup>9,10</sup> [<sup>11</sup>C]diacyl-glycerol,<sup>11,12</sup> and [<sup>11</sup>C]arachidonic acid.<sup>13,14</sup> Other efforts to imaging signal transduction processes with PET that have been limited to evaluation in experimental animal models include the use of fluorine-18 (<sup>18</sup>F; half-life = 109.7 min) labeled FDG to study the protein kinase A (PKA)/cAMP pathway,<sup>15</sup> [<sup>11</sup>C]- and [<sup>18</sup>F]-forskolin for imaging adenylyl cyclase,<sup>16,17</sup> [<sup>11</sup>C]-labeled phorbol esters<sup>18,19</sup> and a [<sup>11</sup>C]-labeled bisindolylmaleimide<sup>20</sup> for imaging protein kinase C, as well as our recent efforts to gain insight into the imaging of glycogen synthase kinase-3 $\beta$  with [<sup>11</sup>C]AR-A014418.<sup>21,22</sup> The goal of this work is to synthesize and evaluate the first radiopharmaceutical for imaging PKA with PET.

Isoquinolinesulfonamide protein kinase inhibitors are among the most widely used inhibitors of the Ser/Thr kinases and are indispensable in cellular and signal transduction research.<sup>23,24</sup> For instance, the protein kinase inhibitors, *N*-(2-aminoethyl)isoquinoline-5-sulfonamide (H-9, **1**) and *N*-(2-(4-bromocinnamylamino)ethyl)-*N*-isoquinoline-5-sulfonamide (H-89, **2**), are frequently used to block signaling pathways in cellular recognition (Fig. 1). The highest selectivity and affinity is found with **2**, a PKA antagonist with IC<sub>50</sub> = 35 nM and 2.5  $\mu$ M for PKA and PKB, respectively.<sup>25</sup> Greater potency of **2** over **1** is attributed to the large bromocinnamyl group which provides an increased number of van der Waals contacts with the protein.<sup>23</sup>

Compound **2** was chosen as a lead candidate for PET radioligand development for the reasons of selectivity, potency and feasibility of chemical modification to incorporate a *N*-methyl group at the sulfonamidic nitrogen. The *N*-methyl group serves as a platform for radio-

labeling of this series of compounds with carbon-11 as potential PET radiopharmaceuticals. Libraries of compounds have been prepared to examine chemical and structural modifications of **2** in order to investigate the affinity and specificity of these derivatives toward PKA and PKB.<sup>25</sup> To our knowledge, the present work is the first to investigate the introduction of a methyl group at the sulfonamidic nitrogen on the affinity of PKA for **1** and **2**. We also studied the effect of further increasing the number of van der Waals contacts of **2** by selectively introducing an additional bromocinnamyl moiety. The lead compound, *N*-(2-(4-bromocinnamylamino)ethyl)-*N*-methyl-isoquinoline-5-sulfonamide (**5**), based on in vitro analysis, was radiolabeled with carbon-11 and evaluated ex vivo in rodent models for cerebral biodistribution.

## 2. Results and discussion

### 2.1. Chemistry

In the present work, structural modifications were made to **1** and **2**, namely the introduction of a methyl group at the sulfonamidic nitrogen, compounds, *N*-(2-aminoethyl)-*N*-methyl-isoquinoline-5-sulfonamide (**4**) and **5**, respectively (Scheme 1). The binding pocket is likely very tight at the 5-isoquinolinesulfonamide moiety as most modifications to this group, including changes to the length of the amino spacer and/or the replacement of the bromocinnamyl moiety with other highly hydrophobic groups, have reduced or abolished inhibition toward PKA.<sup>25</sup> It appears that the amino protons are important to maintain an inhibitory effect through hydrogen bonding interactions, and the relative position of these two centers are crucial.<sup>25</sup> The possibility that one of the hydrogen bonds actively participates in the interaction needs to be further elucidated and can be explored by derivatization at one of the basic nitrogen centers. It was postulated that the introduction of a methyl group at the sulfonamidic nitrogen on compounds **1** and **2** should be a small enough structural change to cause minimal reduction in potency toward PKA, and provide a foundation for radiolabeling with carbon-11.

The *N*-methyl derivative of **1** (H-9), compound **4**, has been investigated as a cardiovascular drug and the synthesis was reported in four steps.<sup>26</sup> We here report a simplified synthesis of **4** by the reaction of isoquinoline-5-sulfonyl chloride with *N*-methylethylenediamine (Scheme 1). Because <sup>1</sup>H and <sup>13</sup>C NMR spectroscopy and HRMS did not unequivocally confirm the presence of the *N*-Me group at the sulfonamidic nitrogen, further characterization was carried out. The structure of **4** was determined by 2-D NMR spectroscopy, namely, ROESY, which showed through-space interaction as cross peaks between aromatic protons and *N*-methyl protons, and by the use of <sup>15</sup>N NMR chemical shifts (obtained by <sup>1</sup>H–<sup>15</sup>N HMBC). The <sup>15</sup>N NMR chemical shifts,  $\delta$  (ppm): –70, –296, and –364 are in close agreement with predicted values of  $-69 \pm 5$ ,  $-291 \pm 12$  and  $-360 \pm 5$  (see Section 3), respectively. In agreement with the thorough NMR characterization of **4**, the X-ray

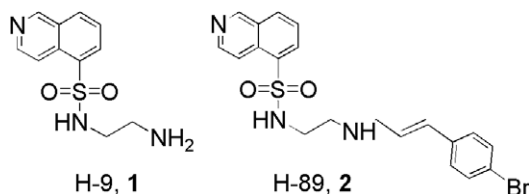
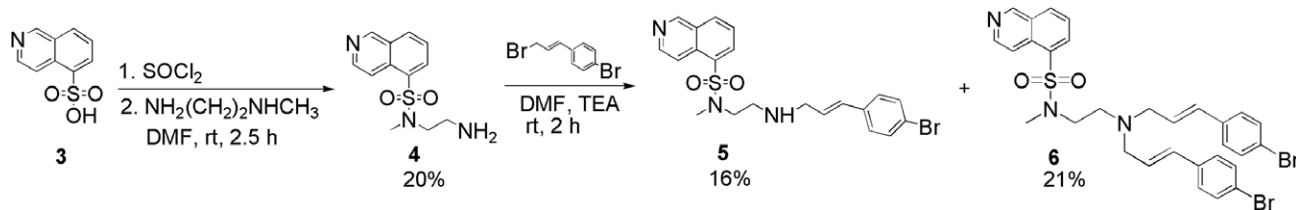


**Figure 1.** Chemical structures of *N*-(2-aminoethyl)isoquinoline-5-sulfonamide (H-9, **1**) and *N*-(2-(4-bromocinnamylamino)ethyl)-*N*-isoquinoline-5-sulfonamide (H-89, **2**).



Scheme 1. Syntheses of compounds 4–6.

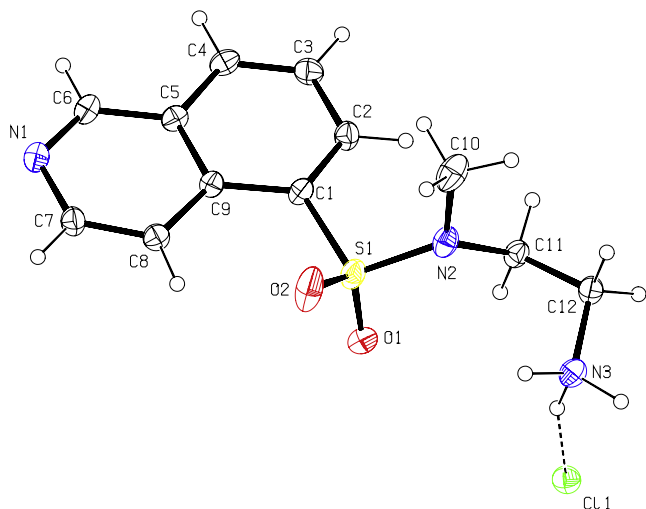


Figure 2. X-ray structure of 4 (hydrochloride salt).

crystal structure of 4 (hydrochloride salt; Fig. 2) unambiguously shows the *N*-methyl group bound to the sulfonamidic nitrogen. Structural mechanisms of inhibitory potency and selectivity have been gained from over 150 kinase and kinase/inhibitor crystal structures that are publicly accessible,<sup>27</sup> and continued efforts should assist in design of protein kinase inhibitors with specific properties.<sup>28</sup>

Derivatives of 2 (H-89) were also prepared. Compounds 5 and *N*-(bis-2-(4-bromocinnamylamino)ethyl)-*N*-methyl-isoquinoline-5-sulfonamide (6) were synthesized in 16% and 21% yields, respectively, by the reaction of 4 with 1-(4-bromophenyl)-1-propen-3-yl bromide<sup>29</sup> and isolated by flash chromatography (Scheme 1). The binding of 2 is described in X-ray crystallographic studies.<sup>23</sup> The large bromocinnamyl group extends 2 to roughly the size of an ATP molecule but cannot mimic any of the properties of a triphosphate. The large Br contributes to van der Waals contacts. The high affinity of 2 compared with 1 is explained by the much larger number of van der Waals contacts to the enzyme. The additional bromocinnamyl group in compound 6 further increases the number of van der Waals contacts to the enzyme and was postulated to have higher affinity toward PKA.

## 2.2. In vitro studies

A preliminary assay to determine relative PKA inhibition was conducted using 20  $\mu$ M of compounds 4–6, with authentic samples of 1 and 2 included for compar-

ison. This assay showed that the *N*-methyl derivatives 4 and 5 display similar potency to 1 and 2, respectively (Fig. 3). Addition of the *N*-methyl group had little effect on potency compared to the parent compounds, and compounds 2 (H-89) and 5 were more potent inhibitors than compounds 1 (H-9) and 4. Interestingly, the dicinnamyl analog, 6, has intermediate potency.

A range of concentrations were used on the most promising compound, 5, and it was found to have an uncorrected  $IC_{50}$  value of 1.28  $\mu$ M under our assay conditions (Fig. 4). The difference between the corrected  $IC_{50}$  for 2 (35 nM)<sup>25</sup> and the higher value in the present work is due to the greater concentration of ATP used (125  $\mu$ M). This was done in order to ensure a closer proximity to physiological levels of ATP, as these ligands are ATP competitive.

## 2.3. Radiochemistry

Radiosynthesis was shown to be reliable and efficient (40 min) for the production of mCi quantities of chemically and radiochemically pure [ $^{11}C$ ]5 (>98%;  $n = 3$ ). In this reaction, 2 (free base) was dissolved in DMF and deprotonated with an equimolar amount of tetrabutylammonium hydroxide (TBAOH) immediately prior to a 5 min reaction at ambient temperature with [ $^{11}C$ ]CH<sub>3</sub>I, using the ‘Loop’ method<sup>30</sup> (Scheme 2). Following methylation, [ $^{11}C$ ]5 was purified by HPLC and

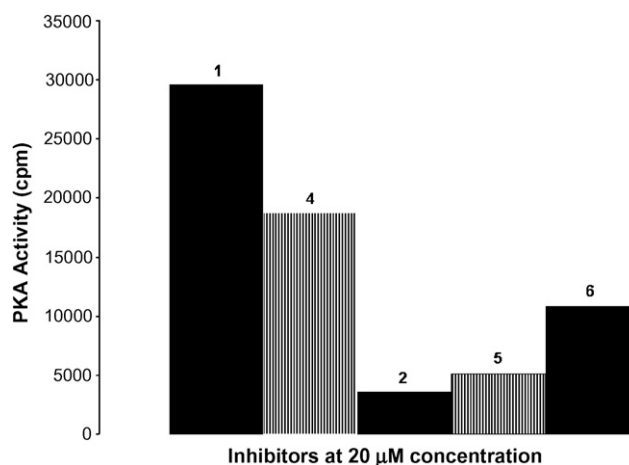
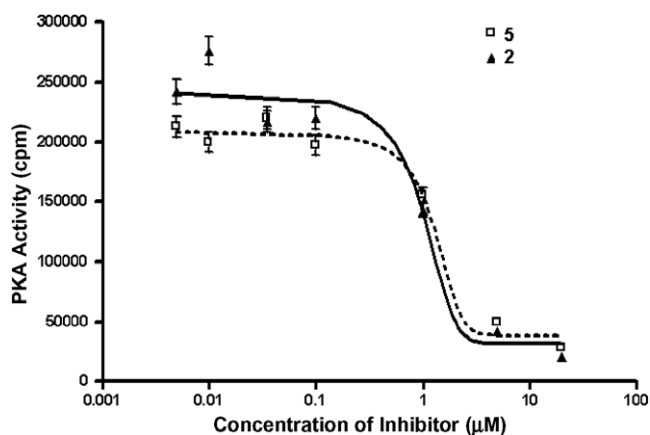


Figure 3. PKA activity for compounds 1, 2, 4, 5, and 6. Purified PKA was assayed against Kemptide substrate in the presence of 20  $\mu$ M of each inhibitor. Positive control, in the absence of inhibitor, showed 27,000 cpm and negative control, the background reading (2400 cpm) was subtracted.



**Figure 4.** Concentration curves for compounds **2** and **5** showing in vitro inhibition of PKA activity (background counts subtracted). Error bars indicate standard deviation. The uncorrected calculated  $IC_{50}$  values in this assay (using 125  $\mu$ M ATP) are 0.94 and 1.28  $\mu$ M, respectively.

formulated in saline.<sup>21</sup> A production of [ $^{11}C$ ]CO<sub>2</sub> resulted in 111 mCi of [ $^{11}C$ ]**5**, ready for injection, corresponding to 32% decay-corrected radiochemical yield, based on [ $^{11}C$ ]CO<sub>2</sub> at the end of bombardment (ca. 65% incorporation from [ $^{11}C$ ]CH<sub>3</sub>I). The specific activity of [ $^{11}C$ ]**5** was 1130 mCi/ $\mu$ mol at the end of synthesis (EOS).<sup>21</sup>

#### 2.4. Ex vivo cerebral biodistribution in rodents

Ex vivo biodistribution studies following the administration of [ $^{11}C$ ]**5** in male Sprague–Dawley rats (257  $\pm$  12 g) were conducted as previously described by our group.<sup>22,23</sup> Rats were injected in the tail vein with a saline solution of [ $^{11}C$ ]**5** and sacrificed at 5, 15, 30, and 60 min after injection ( $n$  = 3 per time point), and brain regions were excised and measured for radioactivity. Blood (trunk) was also collected for radioactivity measurement. Figure 5 shows the distribution of activity for [ $^{11}C$ ]**5** in six regions of the rat brain (cerebellum, hippocampus, striatum, cortex, hypothalamus, and thalamus), the remainder of the brain, and whole blood after injection of the radiotracer. Homogenous distribution of low-levels of radioactivity (<0.2%ID/g) was seen in all brain regions at all time points. A blocking study with a pre-administration of **2** did not appreciably reduce the signal.

Ex vivo measurement of radioactivity in tissue after the injection of [ $^{11}C$ ]**5** in rats clearly indicates that this compound cannot be used to study PKA in the CNS with PET. Successful radiotracers for imaging the central ner-

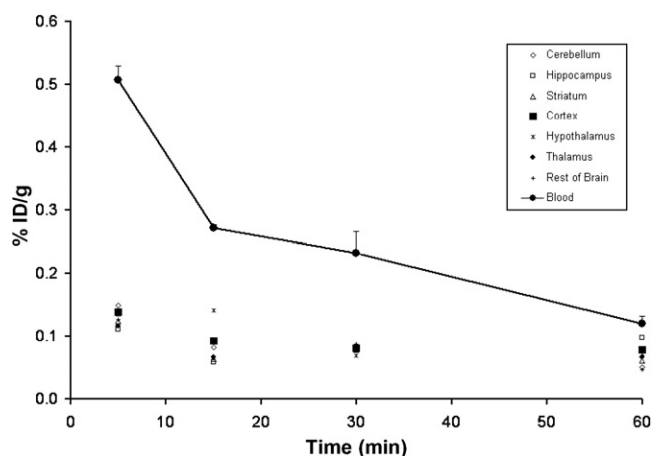
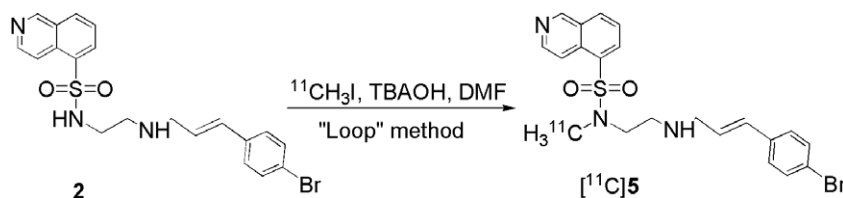


**Figure 5.** Distribution of radioactivity in rat brain regions and whole blood at 5, 15, 30, and 60 min ( $n$  = 3 per time point; mean  $\pm$  SD shown) following tail vein injection of [ $^{11}C$ ]**5** is shown. Homogenous distribution of low levels of radioactivity was seen in all brain regions at all time points.

vous system typically express a %ID/g of tissue  $\geq$  0.5% in rodent brain.<sup>31</sup> The low levels of radioactivity in the brain following the administration of [ $^{11}C$ ]**5** were unexpected considering its measured log  $P$  value between 1-octanol and 0.02 M phosphate buffer at pH 7.4, using a previously described procedure,<sup>32</sup> was  $2.93 \pm 0.02$ , a value which is typical of many brain penetrating compounds.<sup>33</sup> Although [ $^{11}C$ ]**5** does not appear to be suitable for studying the CNS with PET, further studies are presently underway in our laboratory and hope to gain further insight into its pharmacological mechanism(s) and investigate the potential role of [ $^{11}C$ ]**5** in monitoring and classifying tumors.<sup>34,35</sup>

#### 2.5. Conclusion

Here we report the synthesis of novel derivatives of isoquinolinesulfonamide-based PKA inhibitors which can be readily radiolabeled for PET. The most promising inhibitor based on in vitro potency, **5**, was successfully labeled with carbon-11 with high radiochemical purity and specific activity. The ex vivo evaluation of [ $^{11}C$ ]**5** in rats indicates that this compound cannot be used to study PKA in the brain with PET. However, [ $^{11}C$ ]**5** has potential applications for PKA imaging in the periphery. Furthermore, the X-ray crystal structure of *N*-(2-aminoethyl)-*N*-methyl-isoquinoline-5-sulfonamide (**4**) should be useful to elucidate the inhibition mechanisms at atomic resolution and guide structure-based, fragment-based, and computer-aided drug design of therapeutic modulators of signaling pathways.



**Scheme 2.** Radiosynthesis of [ $^{11}C$ ]**5**.



### 3. Experimental

#### 3.1. General methods

Chemical reagents and solvents were obtained from commercially available sources and were used as received without further purification unless indicated. H-89 was obtained as the free base from Toronto Research Chemicals. All other chemicals were obtained from Aldrich or Caledon. Chemical yields were not optimized. For radiochemistry, THF was freshly distilled under nitrogen from  $\text{LiAlH}_4$ , while DMF was distilled under vacuum from barium oxide and stored over 4 Å molecular sieves prior to use.

A Scanditronix MC 17 cyclotron was used for the radionuclide production. Purifications and analyses of radioactive mixtures were performed by HPLC with an in-line UV (254 nm) detector in series with a NaI crystal radioactivity detector (radiosynthesis and QC). Isolated radiochemical yields were determined with a dose calibrator (Capintec CRC-712M).

Electrospray ionization mass spectrometry was conducted with MDS Sciex QStar mass spectrometer to obtain the HRMS. Elemental Analysis was performed by the Analytical Laboratory for Environmental Science Research and Training, University of Toronto, using a PerkinElmer Model 2400II CHN analyzer with PerkinElmer AD-6 autobalance. Samples were calibrated against thermal standard acetanilide (C: 71.09, H: 6.71, N: 10.36) before and after analysis.

One-dimensional proton and carbon-13 NMR spectra were recorded at 25 °C on a Varian Mercury 300 MHz spectrometer with an autoswitchable H/F/C/P 5-mm probe with gradients. The samples were dissolved in  $\text{CDCl}_3$  (Cambridge Isotope Laboratories, Inc.). Chemical shifts were reported using tetramethylsilane (TMS, 0.00 ppm) as an internal standard for  $^1\text{H}$  NMR or by referencing on the  $\text{CHCl}_3$  impurity (at 7.26 ppm) and correcting to TMS. For the  $^{13}\text{C}$  NMR, referencing was done relative to  $\text{CDCl}_3$  (referencing at 77.0 ppm) and correcting the shifts to TMS.

Transverse-ROESY was acquired on a 400 MHz 3 channel Varian NMR System spectrometer equipped with a z-axis gradient driver and variable temperature control. The probe used was a Varian ATB 5-mm direct broadband probe. Spectra were recorded in the phase sensitive mode using  $2 \times 256$  increments in F1. Each increment was obtained in 32 scans and an acquisition time of 246 ms and a pulse width of 5.5  $\mu\text{s}$ . The spectral window was 4166.7 Hz. A mixing time of 400 ms was used. Gaussian apodization was used in the processing.

The  $^1\text{H}$ – $^{15}\text{N}$  (heteronuclear multiple bond correlation; HMBC) was run on a 500 MHz 3 channel Varian Unity NMR spectrometer equipped with a z-axis gradient driver and variable temperature control. The probe used was a Varian PFG 5-mm indirect broadband probe. The HMBC experiments were run in the absolute value mode using 1024 increments in F1, linear

predicting to 2048 increments and zero filling to 4096. The pulse field gradient version of the HMBC was used. The spectral window in F1 was 22,805 Hz and in F2, 4950 Hz. 16 scans per increment with a relaxation delay of 2 s were used. The acquisition time was 206 ms with a proton pulse width of 5.5  $\mu\text{s}$ , and the nitrogen pulse was 30.0  $\mu\text{s}$ . A low pass filter set to 90 Hz was used in the HMBC and the long range multiple bond correlation was observed for a value of 15 Hz. Sinebell apodization was used in the processing. No decoupling of  $^{15}\text{N}$  was used. Predicted  $^{15}\text{N}$  NMR spectra were obtained using ACD/I-Lab Web Service. Please refer to <http://www.acdlabs.com/ilab/> for more information.

X-ray crystal structure data were collected on a Bruker-Nonius Kappa-CCD diffractometer using monochromated  $\text{Mo-K}\alpha$  radiation and were measured using a combination of  $\phi$  scans and  $\omega$  scans with  $\kappa$  offsets to fill the Ewald sphere. The data were processed using the Denzo-SMN package. Absorption corrections were carried out using SORTAV. The structure was solved and refined using SHELXTL V6.1 for full-matrix least-squares refinement that was based on  $F^2$ .

All animal experiments were carried out under humane conditions, with approval from the Animal Care Committee at the Centre for Addiction and Mental Health, and in accordance with the guidelines set forth by the Canadian Council on Animal Care.

#### 3.2. *N*-(2-Aminoethyl)-*N*-methyl-isoquinoline-5-sulfonamide (4)

A mixture of 5-isoquinolinesulfonic acid, **3** (10 g, 48 mmol),  $\text{SOCl}_2$  (75 g, 630 mmol), and DMF (200  $\mu\text{L}$ ) was refluxed for 2 h, and the resulting solution was evaporated. The residue was suspended in  $\text{CH}_2\text{Cl}_2$  (30 mL), filtered, and washed with two portions of  $\text{CH}_2\text{Cl}_2$  (20 mL). The precipitate was collected and dried under reduced pressure to remove the solvent, yielding crude crystalline 5-isoquinolinesulfonyl chloride hydrochloride (9.79 g, 90%). The compound was used as is in the subsequent reaction.

To an ice-cold aqueous (15 mL) solution of crude 5-isoquinolinesulfonyl chloride hydrochloride (5 g, 19 mmol) was added slowly  $\text{NaHCO}_3$  (1.58 g, 18.9 mmol) with stirring. The resulting solution was extracted twice with  $\text{CH}_2\text{Cl}_2$  ( $2 \times 25$  mL). The combined extracts were dried ( $\text{Na}_2\text{SO}_4$ ) and added to a  $\text{CH}_2\text{Cl}_2$  solution (5 mL) of *N*-methylethylenediamine (5 mL, 57 mmol) at 0 °C. The solution was stirred for 2.5 h with warming to room temperature, washed with water (5 mL), and evaporated. The residue was purified by silica gel column chromatography eluting with 10% methanol in chloroform ( $R_f = 0.2$  in 20 % methanol: chloroform) to provide **4** as an oil in 20% yield (1.20 g). Treatment with ethereal HCl (1 M) afforded the hydrochloride salt as a yellow semi-solid. X-ray quality crystals were obtained from the salt of **4** by slow evaporation of a solution in  $\text{Et}_2\text{O}$  and  $\text{CHCl}_3$  (50:50, v/v) containing 5% MeOH.

$^1\text{H}$  NMR ( $\text{CDCl}_3$ , 300 MHz)  $\delta$ : 9.35 (d,  $J = 0.8$  Hz, 1H, isoquinoline *H*-1), 8.70 (d,  $J = 6.2$  Hz, 1H, isoquinoline, *H*-3), 8.50 (d,  $J = 6.2$  Hz, 1H, isoquinoline *H*-4), 8.38 (dd,  $J = 7.4$  Hz,  $J = 1.1$  Hz, 1H, isoquinoline *H*-6), 8.22 (m, 1H, isoquinoline *H*-8), 7.72 (dd, 1H,  $J = 7.6$  Hz,  $J = 8.6$  Hz isoquinoline *H*-7), 3.24 (t,  $J = 6.1$  Hz, 2H,  $\text{CH}_2$ ), 2.88 (t,  $J = 6.1$  Hz, 2H,  $\text{CH}_2$ ), 2.86 (s, 3H, N- $\text{CH}_3$ ), 1.46 (br s, 2H,  $\text{NH}_2$ ).

$^{13}\text{C}$  NMR ( $\text{CDCl}_3$ , 300 MHz)  $\delta$ : 153.5, 145.4, 133.9, 133.8, 132.1, 129.4, 126.1, 117.8, 53.1, 39.9, 34.8.

$^{15}\text{N}$  NMR ( $^1\text{H}$ – $^{15}\text{N}$  HMBC,  $\text{CDCl}_3$ , 500 MHz):  $\delta$ : –70, –296, –364.

HRMS (ESI, positive mode;  $m/z$ , %) Calculated for mass  $\text{C}_{12}\text{H}_{15}\text{N}_3\text{O}_2\text{S}$   $\text{H}^+$ : 266.0957 amu. Found 266.0966.

Anal. ( $\text{C}_{12}\text{H}_{16}\text{ClN}_3\text{O}_2\text{S}$ ) Calcd: C, 47.76; H, 5.34; Cl, 11.75; N, 13.92; O, 10.60; S, 10.62. Found: C, 49.48; H, 5.39; N, 12.52.

Crystal structure of **4**:  $\text{C}_{12}\text{H}_{16}\text{ClN}_3\text{O}_2\text{S}$ ,  $T = 150(1)$  K, monoclinic,  $P\ 2_1/c$ ,  $Z = 4$ ,  $a = 11.9175(5)$  Å,  $b = 16.7471(13)$  Å,  $c = 7.1327(8)$  Å,  $\alpha = 90^\circ$ ,  $\beta = 102.495(5)^\circ$ ,  $\gamma = 90^\circ$   $V = 1389.9(2)$  Å<sup>3</sup>,  $R_1 = 0.0539$ ,  $wR_2 = 0.1330$  for  $I > 2\sigma(I)$ , GOF on  $F^2 = 1.057$ . Crystallographic data (excluding structure factors) for the structure in this paper has been deposited with the Cambridge Crystallographic Data Centre as supplementary publication number CCDC 667990.

### 3.3. *N*-(2-(4-Bromocinnamylamino)ethyl)-*N*-methyl-isoquinoline-5-sulfonamide (**5**) and *N*-(2-(bis-(4-bromocinnamyl)amino)ethyl)-*N*-methyl-isoquinoline-5-sulfonamide (**6**)

1-(4-Bromophenyl)-1-propen-3-yl bromide was prepared in three steps by a literature procedure,<sup>29</sup> with minor modifications. *N*-Methyl-(2-aminoethyl)-5-isoquinolinesulfonamide (**4**) (0.50 g, 1.9 mmol) was dissolved in DMF (4 mL), and *p*-bromocinnamyl bromide (524 mg, 1.9 mmol) was added to this mixture followed by the addition of triethylamine (265  $\mu\text{L}$ , 1.9 mmol). The reaction was stirred at ambient temperature and monitored by TLC. The reaction was complete after 2 h as noted by the disappearance of cinnamyl bromide. The reaction mixture was partitioned between  $\text{CHCl}_3$  (250 mL) and water ( $3 \times 20$  mL). The organic layer was dried over  $\text{Na}_2\text{SO}_4$ , filtered, and solvent removed under reduced atmosphere. The crude extract was purified by column chromatography on silica gel eluting with 5% methanol in chloroform. The process gave **5** as yellow oil ( $R_f = 0.1$  in  $\text{CHCl}_3/\text{EtOH}$  (95:5)) in 16% yield (138.5 mg). The disubstituted product, **6**, was isolated ( $R_f = 0.4$  in  $\text{CHCl}_3/\text{EtOH}$  (95:5)) in 21% yield (262 mg). Treatment with ethereal HCl (1 M) afforded the hydrochloride salts of **5** and **6** as an orange crystalline solid and thick oil, respectively.

Characterization of **5**: mp 78–80 °C.  $^1\text{H}$  NMR ( $\text{CDCl}_3$ , 300 MHz)  $\delta$ : 9.31 (s, 1H, isoquinoline *H*-1), 8.66 (d,  $J = 6.1$  Hz, 1H, isoquinoline *H*-3), 8.49 (d,  $J = 6.1$  Hz,

1H, isoquinoline, *H*-4), 8.36 (dd,  $J = 7.4$  Hz,  $J = 0.9$  Hz, 1H, isoquinoline *H*-8), 8.18 (d,  $J = 8.2$  Hz, 1H, isoquinoline *H*-6), 7.68 (t,  $J = 7.9$  Hz, 1H, isoquinoline *H*-7), 7.42 (d,  $J = 8.5$  Hz, 2H, Ph-*H*), 7.20 (d,  $J = 8.5$  Hz, 2H, Ph-*H*), 6.43 (d,  $J = 16$  Hz, 1H, Ph- $\text{CH}=\text{CHCH}_2$ ), 6.19 (dt,  $J = 16$  Hz,  $J = 6.2$  Hz, 1H, Ph- $\text{CH}=\text{CHCH}_2$ ), 4.72 (br s, 1H,  $\text{NH}$ ), 3.38 (d,  $J = 6.3$  Hz, 2H, Ph- $\text{CH}=\text{CHCH}_2$ ), 3.34 (t,  $J = 6.3$  Hz, 2H,  $\text{MeNCH}_2\text{CH}_2$ ), 2.87 (s, 3H, N- $\text{CH}_3$ ), 2.85 (t,  $J = 6.3$  Hz, 2H,  $\text{MeCH}_2\text{CH}_2$ ).

$^{13}\text{C}$  NMR ( $\text{CDCl}_3$ , 300 MHz)  $\delta$ : 153.5, 145.4, 135.8, 133.83, 133.81, 133.3, 132.0, 131.9, 131.8, 131.2, 129.3, 128.0, 127.9, 126.1, 121.5, 117.9, 51.2, 49.5, 46.3, 35.2.

HRMS (ESI, positive mode;  $m/z$ , %): Calculated for mass  $\text{C}_{21}\text{H}_{22}\text{BrN}_3\text{O}_2\text{S}$   $\text{H}^+$ : 460.0688 amu. Found 460.0692.

Anal. ( $\text{C}_{21}\text{H}_{24}\text{Br}_2\text{Cl}_2\text{N}_3\text{O}_2\text{S}$ ) Calcd: C, 47.29; H, 4.54; Br, 14.98; Cl, 13.30; N, 7.88; O, 6.00; S, 6.01. Found: C, 46.91; H, 4.36; N, 6.69.

Characterization of **6**:  $^1\text{H}$  NMR ( $\text{CDCl}_3$ , 300 MHz)  $\delta$ : 9.31 (d,  $J = 0.7$  Hz, 1H, isoquinoline *H*-1), 8.62 (d,  $J = 6.2$  Hz, 1H, isoquinoline *H*-3), 8.45 (m, 1H, isoquinoline *H*-4), 8.32 (dd,  $J = 7.4$  Hz,  $J = 1.2$  Hz, 1H, isoquinoline *H*-8), 8.13 (m, 1H, isoquinoline *H*-6), 7.61 (dd,  $J = 7.4$  Hz,  $J = 8.5$  Hz, 1H, isoquinoline *H*-7), 7.42 (d,  $J = 8.5$  Hz, 4H, Ph-*H*), 7.20 (d,  $J = 8.5$  Hz, 4H, Ph-*H*), 6.45 (d,  $J = 16$  Hz, 2H, 2 (Ph- $\text{CH}=\text{CHCH}_2$ )), 6.19 (dt,  $J = 16$  Hz,  $J = 6.6$  Hz, 2H, 2 (Ph- $\text{CH}=\text{CHCH}_2$ )), 3.34 (t,  $J = 6.7$  Hz, 2H,  $\text{MeNCH}_2\text{CH}_2$ ), 3.27 (d,  $J = 6.4$  Hz, 4H, 2 (Ph- $\text{CH}=\text{CHCH}_2$ )), 2.83 (s, 3H, N- $\text{CH}_3$ ), 2.71 (t,  $J = 6.7$  Hz, 2H,  $\text{MeNCH}_2\text{CH}_2$ ).

$^{13}\text{C}$  NMR ( $\text{CDCl}_3$ , 300 MHz)  $\delta$ : 153.5, 145.4, 135.9, 133.9, 133.7, 133.6, 132.0, 131.9, 129.4, 128.1, 126.0, 121.5, 117.9, 57.0, 51.5, 48.1, 35.1.

HRMS (ESI, positive mode;  $m/z$ , %): Calculated for mass  $\text{C}_{30}\text{H}_{29}\text{Br}_2\text{N}_3\text{O}_2\text{S}$   $\text{H}^+$ : 654.0419 amu. Found 654.0429.

Anal. ( $\text{C}_{30}\text{H}_{31}\text{Br}_2\text{Cl}_2\text{N}_3\text{O}_2\text{S}$ ) Calcd: C, 49.47; H, 4.29; Br, 21.94; Cl, 9.73; N, 5.77; O, 4.39; S, 4.40. Found: C, 49.39; H, 4.15; N, 5.50.

### 3.4. In vitro studies

The radioactive assays for PKA inhibition followed a literature procedure<sup>25</sup> with minor modifications. The assay contained 20 mM MOPS, pH 7.2, 5.0 mM EGTA, 25 mM  $\beta$ -glycerophosphate, 1 mM sodium orthovanadate, 1 mM DTT, 125  $\mu\text{M}$  [ $\gamma$ - $^{32}\text{P}$ ]ATP, 18 mM  $\text{MgCl}_2$  and 2.5  $\mu\text{g mL}^{-1}$  PKA, 100  $\mu\text{M}$  of Kemptide and the inhibitory compounds dissolved in DMSO.

The preliminary screening assays involved the incorporation of phosphate from [ $\gamma$ - $^{32}\text{P}$ ]ATP into a synthetic heptapeptide substrate and the separation of the peptide from unincorporated radiolabel using P-81 phosphocellulose paper by the modification of the literature procedure for binding assay with Kemptide.<sup>36</sup>

### 3.5. Radiochemistry

In a 17 MeV cyclotron, 1% O<sub>2</sub> in N<sub>2</sub> was bombarded with 45  $\mu$ A proton beam current. Compound **2** (0.7 mg, 1.6  $\mu$ mol) was dissolved in 78  $\mu$ L of DMF and 1.6  $\mu$ L of a 1.0 M solution of TBAOH in methanol was added prior to a 5 min at room temperature reaction with [<sup>11</sup>C]iodomethane using the ‘Loop’ method.<sup>20</sup> Reverse phase semi-preparative HPLC (Phenomenex C-18 Luna, 250  $\times$  10 mm, 10  $\mu$ m) was performed using a mobile phase consisting of CH<sub>3</sub>CN/H<sub>2</sub>O (40:60 v/v) + 0.1 N ammonium formate (AF) at a flow rate of 9 mL min<sup>-1</sup> to separate [<sup>11</sup>C]**5** ( $t_R$  = 13.7 min) from unreacted **2** ( $t_R$  = 7.2 min) and undesired byproducts. The product eluting at 13.7 min was led into a rotary evaporation flask and heated to dryness at 70 °C, under vacuum. The product was dissolved in 0.5 mL of ethanol and 9.5 mL saline and transferred into a vial containing 1 mL of 8.4% sodium bicarbonate. The pH of the final solution was between 7 and 8. Analytical HPLC was performed using a C-18 column (Phenomenex Prodigy ODS-Prep, 250  $\times$  4.6 mm, 10  $\mu$ m) eluted with CH<sub>3</sub>CN/H<sub>2</sub>O (50:50 v/v) + 0.1 N AF using a flow rate of 2 mL min<sup>-1</sup>. Authentic **5** co-eluted with the <sup>11</sup>C-labeled product under these conditions ( $t_R$  = 3.1 min) and under several different analytical HPLC conditions (mobile and stationary phases, pHs and wavelengths). The formulated product does not undergo any significant radiolysis.

### 3.6. Ex vivo biodistribution in rodents

Ex vivo biodistribution studies following the administration of [<sup>11</sup>C]**5** in unanesthetized male Sprague–Dawley rats (257  $\pm$  12 g) were conducted as previously described by our group.<sup>37,21</sup> Briefly, rats received ca. 1 mCi (at the time of the first injection; 14 min after EOS) of high specific activity [<sup>11</sup>C]**5** in 0.3 mL of buffered saline via the tail vein and were sacrificed by decapitation at 5, 15, 30, and 60 min after injection ( $n$  = 3 per time point). The brains were removed and regions of interest (striatum, thalamus, hypothalamus, hippocampus, cortex, cerebellum and rest of brain) were excised, blotted, and weighed, while blood was collected from the trunk in a heparinized tube for radioactivity measurement, as previously described.<sup>37</sup> A blocking study was repeated, as described above, except that the rats ( $n$  = 6 per group) were pre-treated with 1 mg/kg of H-89 (group 1) or saline (group 2), and sacrificed at 60 min after the injection of [<sup>11</sup>C]**5**.

### Acknowledgments

The authors thank Patrick McCormick and Jun Parkes for their expertise with the biological studies, and Winston Stableford for technical assistance with the radiochemistry. We also thank Dr. Alan Lough, Dr. Alex Young, and Dr. Tim Burrow from the Department of Chemistry, University of Toronto for their expertise with X-ray crystallography, mass spectrometry, and NMR spectroscopy, respectively. Financial support for this work was provided by the Canadian Society of Nu-

clear Medicine and GE Healthcare in the form of a Radiant Program Young Investigator Award (N.V.) and the University of Toronto.

### References and notes

- Cohen, P. *Nat. Rev. Drug Disc.* **2002**, *1*, 309.
- Liao, J. J. *J. Med. Chem.* **2007**, *50*, 409.
- Skalhegg, B. S.; Tasken, K. *Front. Biosci.* **2000**, *5*, D678.
- Taylor, S. S.; Kim, C.; Vigil, D.; Haste, N. M.; Yang, J.; Wu, J.; Anand, G. S. *Biochim. Biophys. Acta* **2005**, *1754*, 25.
- Duman, R.; Heninger, G.; Nestler, E. *Arch. Gen. Psych.* **1997**, *54*, 597.
- Dwivedi, Y.; Rizavi, H. S.; Shukla, P. K.; Lyons, J.; Faludi, G.; Palkovits, M.; Sarosi, A.; Conley, R. R.; Roberts, R. C.; Tamminga, C. A.; Pandey, G. N. *Biol. Psychiatry* **2004**, *55*, 234.
- Dwivedi, Y.; Conley, R. R.; Roberts, R. C.; Tamminga, C. A.; Pandey, G. N. *Am. J. Psychiatry* **2002**, *159*, 66.
- Fowler, J. S.; Wolf, A. P. *Acc. Chem. Res.* **1997**, *30*, 181.
- Lourenco, C. M.; DaSilva, J. N.; Warsh, J. J.; Wilson, A. A.; Houle, S. *Synapse* **1999**, *31*, 41.
- DaSilva, J. N.; Lourenco, C. M.; Meyer, J. H.; Hussey, D.; Potter, W. Z.; Houle, S. *Eur. J. Nucl. Med. Mol. Imaging* **2002**, *29*, 1680.
- Imahori, Y.; Fujii, R.; Ueda, S.; Matsumoto, K.; Wakita, K.; Ido, T.; Nariai, T.; Nakahashi, H. *J. Nucl. Med.* **1992**, *33*, 413.
- Matsumoto, K.; Imahori, Y.; Fujii, R.; Ohmori, Y.; Sekimoto, T.; Ueda, S.; Mineura, K. *J. Nucl. Med.* **1999**, *40*, 1590.
- Channing, M. A.; Simpson, N. J. *Labelled Compd. Radiopharm.* **1993**, *33*, 541.
- Giovacchini, G.; Chang, M. C.; Channing, M. A.; Toczek, M.; Mason, A.; Bokde, A. L.; Connolly, C.; Vuong, B. K.; Ma, Y.; Der, M. G.; Doudet, D. J.; Herscovitch, P.; Eckelman, W. C.; Rapoport, S. I.; Carson, R. E. *J. Cereb. Blood Flow Metab.* **2002**, *22*, 1453.
- Hosoi, R.; Matsumura, A.; Mizokawa, S.; Tanaka, M.; Nakamura, F.; Kobayashi, K.; Watanabe, Y.; Inoue, O. *Brain Res.* **2005**, *1039*, 199.
- Sasaki, T.; Enta, A.; Nozaki, T.; Ishii, S.; Senda, M. *J. Nucl. Med.* **1993**, *34*, 1944.
- Kiesewetter, D. O.; Sassaman, M. B.; Robbins, J.; Jagoda, E. M.; Carson, R. E.; Appel, N. M.; Sutkowski, E.; Herscovitch, P.; Braun, A.; Eckelman, W. C. *J. Fluorine Chem.* **2000**, *101*, 297.
- Imahori, Y.; Fujii, R.; Ido, T.; Hirakawa, K.; Nakahashi, H. *J. Labelled Compd. Radiopharm.* **1989**, *27*, 1025.
- Ohmori, Y.; Imahori, Y.; Ueda, S.; Fujii, R.; Ido, T.; Wakita, K.; Nakahashi, H. *J. Nucl. Med.* **1993**, *34*, 431.
- Takahishi, K.; Kudo, K.; Okada, M.; Yanamoto, K.; Hatori, A.; Irie, T.; Suzuki, K.; Miura, S. *J. Labelled Compd. Radiopharm.* **2007**, *50*, S398.
- Vasdev, N.; Garcia, A.; Stableford, W. T.; Young, A. B.; Meyer, J. H.; Houle, S.; Wilson, A. A. *Bioorg. Med. Chem. Lett.* **2005**, *15*, 5270.
- Vasdev, N.; Wilson, A. A.; Houle, S.; Lough, A. J. *Acta Cryst.* **2007**, *E63*, o1653.
- Engh, R. A.; Girod, A.; Kinzel, V.; Huber, R.; Bossemeyer, D. *J. Biol. Chem.* **1996**, *271*, 26157.
- Collins, I.; Caldwell, J.; Fonseca, T.; Donald, A.; Bave-tsias, V.; Hunter, L. J. K.; Garrett, M. D.; Rowlands, M. G.; Aherne, G. W.; Davies, T. G.; Berdini, V.; Woodhead, S. J.; Davis, D.; Seavers, L. C. A.; Wyatt, P. G.

- Workman, P.; McDonald, E. *Bioorg. Med. Chem.* **2006**, *14*, 1255.
25. Reuveni, H.; Livnah, N.; Geiger, T.; Klein, S.; Ohne, O.; Cohen, I.; Benhar, M.; Gellerman, G.; Levitzki, A. *Biochemistry* **2002**, *41*, 10304.
26. Morikawa, A.; Sone, T.; Asano, T. *J. Med. Chem.* **1989**, *32*, 42.
27. Weinmann, H.; Metternich, R. *Chembiochem* **2005**, *6*, 455.
28. Davies, T. G.; Verdonk, M. L.; Graham, B.; Saalau-Bethell, S.; Hamlett, C. C. F.; McHardy, T.; Collins, I.; Garrett, M. D.; Workman, P.; Woodhead, S. J.; Jhoti, H.; Barford, D. *J. Mol. Biol.* **2007**, *367*, 882.
29. Hammond, M. L.; Zambias, R. A.; Chang, M. N.; Jensen, N. P.; McDonald, J.; Thompson, K.; Boulton, D. A.; Kopka, I. E.; Hand, K. M.; Opas, E. E., et al. *J. Med. Chem.* **1990**, *33*, 908.
30. Wilson, A. A.; Garcia, A.; Jin, L.; Houle, S. *Nucl. Med. Biol.* **2000**, *27*, 529.
31. Wong, D. F.; Pomper, M. G. *Mol. Imaging Biol.* **2003**, *5*, 350.
32. Wilson, A. A.; Jin, L.; Garcia, A.; DaSilva, J. N.; Houle, S. *Appl. Radiat. Isot.* **2001**, *54*, 203.
33. Waterhouse, R. N. *Mol. Imaging Biol.* **2003**, *5*, 376.
34. Nesterova, M. V.; Cho-Chung, Y. S. *Ann. N.Y. Acad. Sci.* **2005**, *1058*, 255.
35. Cho-Chung, Y. S.; Nesterova, M. V. *Ann. N.Y. Acad. Sci.* **2005**, *1058*, 76.
36. Gienbycz, M. A.; Diamond, J. *Biochem. Pharmacol.* **1990**, *39*, 271.
37. Wilson, A. A.; DaSilva, J. N.; Houle, S. *Nucl. Med. Biol.* **1996**, *23*, 141.